INSTITUTE OF PHYSICS PUBLISHING JOURNAL OF PHYSICS: CONDENSED MATTER

J. Phys.: Condens. Matter **15** (2003) 6671–6681 PII: S0953-8984(03)64055-5

Magnetic and optical properties and electron paramagnetic resonance of gadolinium-containing oxide glasses

J Kliava[1,6], I S Edelman[2], A M Potseluyko[2], E A Petrakovskaja[2], R Berger[1], I Bruckental[3], Y Yeshurun[3], A V Malakhovskii[4] and T V Zarubina[5]

[1] CPMOH, Université Bordeaux-I, 33405 Talence Cedex, France
[2] L V Kirensky Institute of Physics SB RAS, Krasnoyarsk 660036, Russia
[3] Bar-Ilan University, Department of Physics, Ramat-Gan 52900, Israel
[4] Bar-Ilan University, Department of Chemistry, Ramat-Gan 52900, Israel
[5] S V Vavilov State Optical Institute, St Petersburg 199034, Russia

E-mail: j.kliava@cpmoh.u-bordeaux1.fr

Received 27 May 2003
Published 26 September 2003
Online at stacks.iop.org/JPhysCM/15/6671

Abstract

Magnetic susceptibility, electron paramagnetic resonance (EPR) and optical absorption have been studied in a glass system $20La_2O_3$–$22Al_2O_3$–$23B_2O_3$–$35(SiO_2 + GeO_2)$ with a part of La_2O_3 substituted by Gd_2O_3 in different concentrations. Positive Weiss constants have been found in more heavily doped glasses and ascribed to clustering of Gd^{3+} ions. Computer simulations of the EPR spectra show that the short-range ordering in the environment of the Gd^{3+} ions is well preserved. The relative distribution widths of the ligand coordinates are less than 2%. In the more heavily doped glasses the EPR spectra are superpositions of signals arising from isolated ions and ferromagnetic clusters. The increase of Gd^{3+} concentration is shown to change substantially the strong optical absorption edge while only small changes of f–f absorption band characteristics are observed. This difference is associated with the different effect of the Gd ion clustering on the mechanisms of the strong absorption in the ultraviolet region and the f–f absorption.

(Some figures in this article are in colour only in the electronic version)

1. Introduction

Gadolinium-containing glasses attract much attention (e.g. see [1–11]) because of the promise of their magnetic and optical properties for technical applications. These properties are

[6] Author to whom any correspondence should be addressed.

determined, on the one hand, by the environment of Gd^{3+} ions and, on the other hand, by the gadolinium concentration and its distribution in the glass matrix. Whereas the local structure of the Gd^{3+} sites seems to be similar in different types of glasses [12], the correlation between the doping level and clustering depends on the glass type and composition. For example, in multicomponent silicate glasses the onset of clustering of Gd^{3+} ions was observed for gadolinium oxide content above 1 mass% [11], while clustering effects were negligible up to $x = 4$ (i.e. 3.1 mass% of Gd_2O_3) in glasses of composition $(40-x)$PbO–$60GeO_2$–xGd_2O_3 [8].

The aim of this work is to obtain systematic data on the structure of Gd^{3+} sites and the distribution of gadolinium ions in the glass at different concentrations. A glass system of composition $20La_2O_3$–$22Al_2O_3$–$23B_2O_3$–$35(SiO_2 + GeO_2)$ with a part of La_2O_3 substituted by Gd_2O_3 has been studied. Such a composition allows the introduction of Gd^{3+} ions in a wide concentration range. Below we present the results obtained using electron paramagnetic resonance (EPR), the field and temperature dependence of magnetization and optical spectroscopy.

2. Experimental details

The glasses were prepared from Gd_2O_3, La_2O_3, Al_2O_3, H_3BO_3, SiO_2 and GeO_2 as starting materials, melted in platinum crucibles at 1400–1500 °C in an electric furnace. The materials were characterized by low impurity contents: that is, maximal Fe content 5×10^{-3} mass% (in Al_2O_3) and maximal Ce content 5×10^{-4} mass% (in La_2O_3); the content of the other impurities was less than 10^{-4} mass%. Four samples, Gd1, Gd2, Gd3 and Gd4, were synthesized with, respectively, $x = 0.1$, 1.0, 5.0 and 10 mass% Gd_2O_3 substituting for the equivalent amounts of La_2O_3. The final mass composition of the glasses (in mass per cent) can be written as $\{xGd_2O_3$–$(51.35 - x)La_2O_3$–$17.4Al_2O_3$–$12.4B_2O_3$–$18.85(SiO_2 + GeO_2)\}$. For such a composition, the environment of the Gd^{3+} ions is expected to remain unchanged when the Gd_2O_3 content increases.

The magnetization measurements as a function of temperature (5–300 K) were made in the field range 0–5 T using a commercial SQUID magnetometer (Quantum Design MPMS-55) with a scan length of 4 cm. The EPR spectra of Gd^{3+} were measured at 78 and 293 K in the X (9.5 GHz) and Q (35 GHz) bands. The optical absorption was measured at room temperature in the wavelength range of 180–600 nm with a UVICON 943 spectrophotometer.

3. Results and discussion

3.1. Magnetization

The field dependence of the gadolinium magnetic moment at 5 K is shown in figure 1. The measurement accuracy with the SQUID magnetometer is 10^{-8} emu, so relative errors in the magnetic moment values are lower than $\pm 0.01\%$. The curves for the Gd1, Gd2 and Gd3 glasses are very similar in shape, while that of the Gd4 glass shows some features in the high-field region. The temperature dependence of the magnetization for all samples is well described by the Curie–Weiss law with a temperature-independent term included to correct for a diamagnetic contribution:

$$M(T) = \left(a + \frac{b}{T - \Theta}\right)B \tag{1}$$

where a and b are constants characterizing relative values of the diamagnetic and paramagnetic contributions to the magnetic moment, B is the applied magnetic field, T is temperature

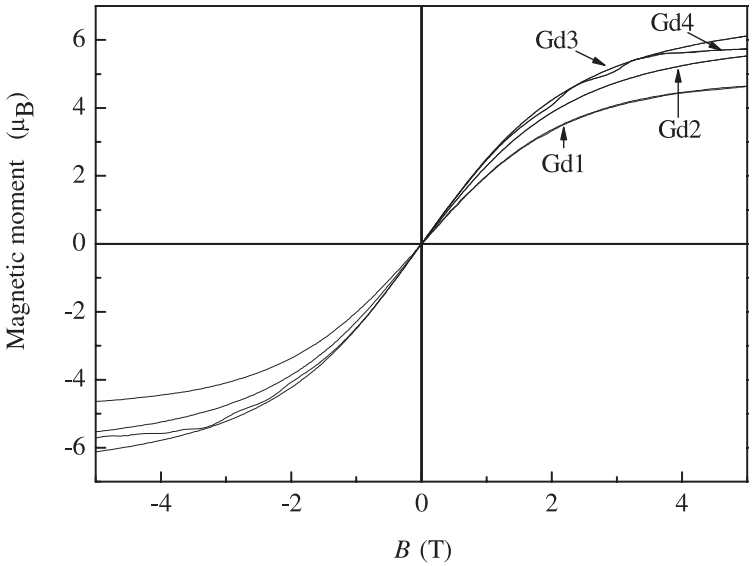

Figure 1. Dependence of the Gd^{3+} magnetic moment (in Bohr magnetons) on the magnetic field for Gd1–Gd4 glasses measured at 5 K.

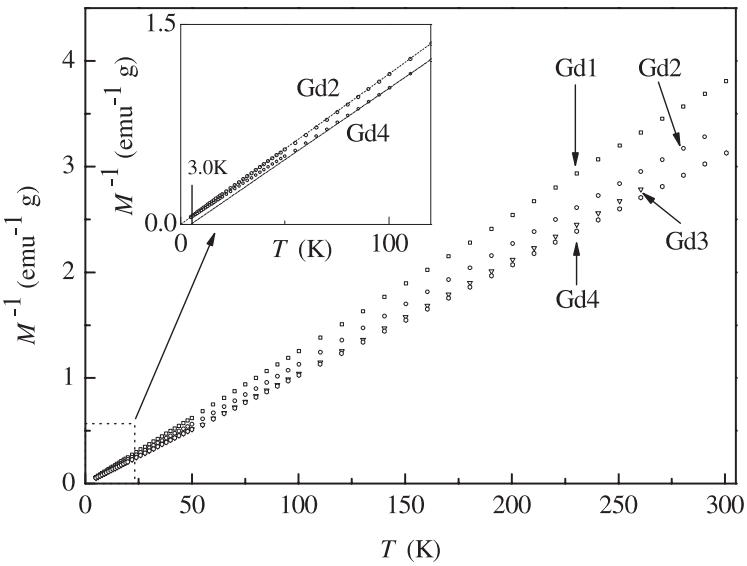

Figure 2. Temperature dependence of the paramagnetic part of inverse magnetization for Gd1–Gd4 glasses measured at $B = 0.2$ T. The inset shows low-temperature data for Gd2 and Gd4 glasses.

and Θ is the Weiss constant. For the glasses with lower gadolinium concentrations (Gd1 and Gd2) the inverse of the paramagnetic part of the magnetization is linear over the whole temperature range studied and is well described assuming $\Theta = 0$. For the glasses with higher gadolinium concentration (Gd3 and Gd4) a deviation from the linear dependence is observed in the low-temperature range, see figure 2. A linear extrapolation of the high-temperature $M^{-1}(T)$ dependence for the Gd3 and Gd4 glasses yields, respectively, $\Theta = 5.0$ and 3.0 K.

Such behaviour indicates the presence of magnetically ordered (presumably, ferromagnetic) clusters.

From figure 2 the b-values are found to be 400, 420, 460 and 480 emu K g^{-1} T^{-1} for Gd1–Gd4, respectively. The a-values are determined by fitting the experimental curves with equation (1) using the Weiss constants given above. For Gd3 and Gd4 at $T < 300$ K the diamagnetic term in (1) is negligibly small compared with the paramagnetic one. For Gd1 and Gd2 we find $a \approx -3.0$ and -0.3 emu g^{-1} T^{-1}, respectively. The first term in (1) is mainly due to the glass matrix; therefore, the values found for a are approximately inversely proportional to the Gd concentration (all calculations were made per gram of Gd).

Note that at higher gadolinium contents, isolated Gd^{3+} ions can coexist with clusters and actual Weiss constants can differ from those obtained by fitting the experimental $M^{-1}(T)$ dependence [13]. Usually, gadolinium-containing glasses have negative Weiss constants [4–6, 8–10], similar to Gd_2O_3 [14]. However, some gadolinium compounds have positive Weiss constants [15], attributed to a strong influence of the environment on the exchange interaction between the Gd^{3+} ions. The positive Weiss constants found here indicate a different environment for gadolinium compared with other types of glasses or Gd_2O_3. In the latter oxide, the Gd^{3+} ions occupy two crystallographic sites, C_2 and C_{3i}, so one must introduce two different exchange constants corresponding to interactions between C_2 and C_{3i} sites and between two C_2 sites [14]. Similarly, in the present case one may infer the presence of several types of gadolinium clusters in the Gd3 and Gd4 glasses. The lower Weiss constant and the features observed in the field dependence of the magnetization, figure 1, for the Gd4 glass, can be tentatively ascribed to the antiferromagnetic nature of some clusters.

From the temperature dependence of magnetization, high-temperature effective magnetic moments μ_{eff} of Gd^{3+} are determined as 7.15, 7.48, 7.60 and $7.74\mu_B$ (μ_B is the Bohr magneton), respectively, for Gd1, Gd2, Gd3 and Gd4. As expected for the $^8S_{7/2}$ ground state configuration, these values are close to the magnetic moment of the free Gd^{3+} ion, $\mu_{\text{eff}} = 7.94\mu_B$, indicating a weak influence of the crystal field (CF) on the magnetic moments. The fact that this influence is clearly less pronounced at higher gadolinium concentrations can be related to a weakening of distortions in the glass network caused by the difference in the radii of the host and the substituting ions (for La^{3+} $r = 1.172$ Å, while for Gd^{3+} $r = 1.078$ Å [16]).

3.2. EPR

Figure 3 shows the X-band EPR spectra for all glasses at 78 and 293 K. Between the liquid nitrogen and room temperatures the spectral shape remains nearly the same, whereas the overall intensities (I) vary in proportion $I_{78\,\text{K}}/I_{293\,\text{K}} = 3.2$, 3.0, 2.0 and 2.4 for the Gd1, Gd2, Gd3, and Gd4 glasses, respectively. Note that the larger intensity ratios in the less doped glasses are consistent with the more rapid increase of the magnetization on lowering the temperature, see figure 2. In the Gd1 and Gd2 glasses, the spectra show well-resolved features at the effective g-values $g_{\text{eff}} = 5.9$, 2.8 and 2.0, characteristic of the so-called U-spectrum [2–5, 9, 10]. In the corresponding Q-band spectra only a relatively narrow single line with $g_{\text{eff}} = 2.0$ is observed.

In comparison with the other above-quoted cases of Gd^{3+} spectra in disordered host matrices, the present glasses are characterized by a lower relative intensity of the $g_{\text{eff}} = 2.0$ feature. For example, for Gd2, $I_{g_{\text{eff}}=2.0}/I_{g_{\text{eff}}=2.8} = 1/3$, while in zeolites this ratio is about 1.0 [2]. We show below that this fact can be accounted for by assuming a larger dispersion of the second-order fine-structure (zero-field-splitting) parameters, corresponding to less ordered Gd^{3+} sites.

In the EPR spectra of Gd2 in comparison with the Gd1 glass, only a slight line broadening is observed. Therefore, the Gd^{3+} ions in these glasses can be considered as isolated in the

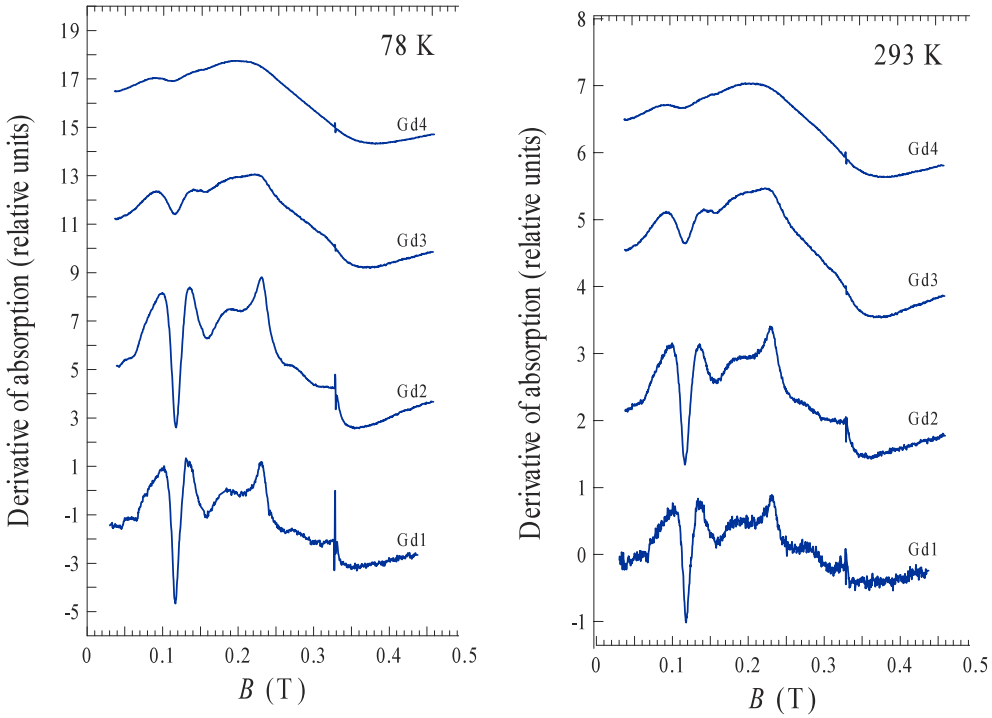

Figure 3. Experimental EPR spectra at 78 K (left) and 293 K (right). All spectral intensities have been normalized with respect to the number of Gd^{3+} ions in the corresponding glasses. The narrow peak at $B \approx 0.328$ T arises from a DPPH marker ($g_{\mathrm{eff}} = 2.0036$).

sense of the absence of clustering. This is in agreement with the temperature dependence of the magnetic susceptibility in these glasses, *vide infra*. On the other hand, in the Gd3 and Gd4 glasses all spectral features are broadened. This broadening is naturally ascribed to dipole–dipole interactions between the Gd^{3+} ions. Meanwhile, in order to account unambiguously for the spectral transformation with the gadolinium concentration, a more quantitative analysis is needed.

The EPR spectra have been numerically simulated by means of an *ab initio* code [17] directly relating the atomic positions in the environment of the paramagnetic ions to the spin Hamiltonian parameters using the superposition model. All the spin Hamiltonian parameters consistent with the low-symmetry sites in glass have been taken into account. However, preliminary simulations have shown that only the Zeeman term (with the g-factor very close to the free-electron value) and the second-order fine-structure terms are really needed. Introducing non-zero values for the remaining parameters only alters the fits of the experimental spectra; therefore, one can conclude that their actual values are very small. The superposition model parameters for the second-order fine-structure terms for Gd^{3+} have been chosen in accordance with [18] as follows: $t_2 = 2.5$ and $\bar{b}_2(R)_0 = -0.2\ \mathrm{cm}^{-1}$ for the reference distance $R_0 = 2.699$ Å.

In order to account for the inherent disorder in the glass, a randomly distorted octahedral environment of Gd^{3+} has been assumed, with the coordination polyhedra subjected to *second-order* random distributions. Such an approach describes both the disorder in the close environment of a paramagnetic ion and the possible presence of sites with different degrees

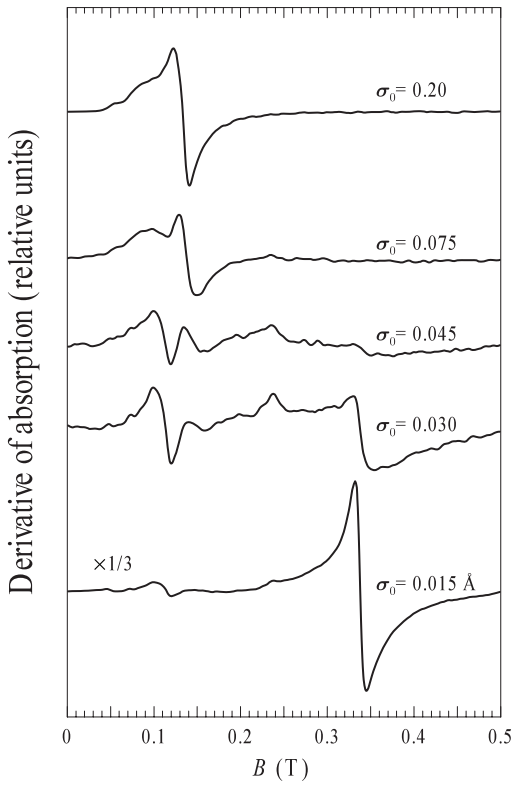

Figure 4. Series of computer-generated Gd^{3+} EPR spectra (see the text for details). The mean distribution widths are indicated alongside the corresponding curves. The rms deviation of σ is 0.012 Å for all the spectra. The intrinsic lineshape is Lorentzian with a 3.5 mT linewidth.

of short-range ordering or of more or less ordered regions in the glass network. To this end, the oxygen sites have been normally distributed around their positions in a perfect octahedron with a metal-to-ligand distance of 2.338 Å (the sum of the octahedral ionic radii for Gd^{3+} and O^{2-} [16]) with a distribution width σ. The σ-value, in turn, has been submitted to a normal distribution with a mean value of σ_0 and an rms deviation of $\Delta\sigma$. The ligand positions have been generated with a Monte Carlo procedure, yielding a Gaussian distribution density by appropriately transforming a uniform distribution obtained using the RANMAR code [19]. Producing the derivatives of absorption spectra with acceptable signal-to-noise ratio required the accumulated absorption of about 1×10^6 'centres'.

As an example, in figure 4 we show a series of computer-generated spectra for different mean distribution widths σ_0. The best fit to the experimental EPR spectra of the Gd1 and Gd2 glasses has been obtained for $\sigma_0 = 0.045$ Å and $\Delta\sigma = 0.012$ Å. (The remaining discrepancy between the experimental and calculated spectra in the field range of about 0.12–0.15 T is due to a superimposed signal arising from traces of Fe^{3+}.) These results indicate that the short-range ordering surrounding the Gd^{3+} ions is fairly well preserved, the relative distribution width of the ligand positions being less than about 2%.

As the possible cause of the overall change of the EPR spectral shapes in the Gd3 and Gd4 glasses one may suggest three different mechanisms, namely, (i) dipole–dipole interactions between the Gd^{3+} ions, (ii) modification of the degree of short-range ordering

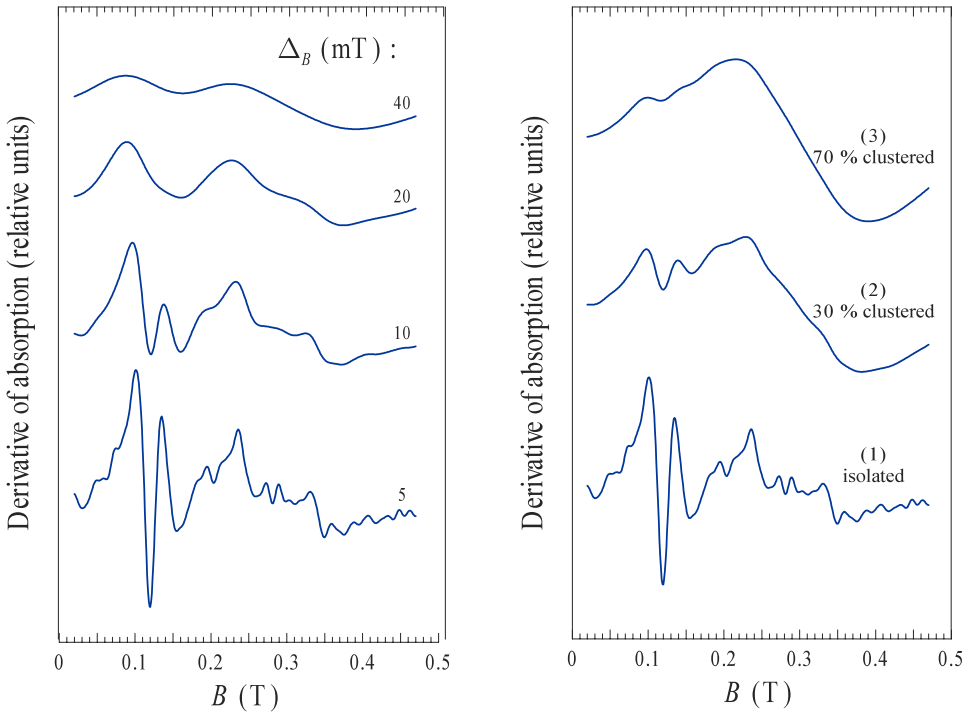

Figure 5. Computer-generated spectra. Left: spectra calculated for $\sigma_0 = 0.045$ Å, $\Delta\sigma = 0.012$ and a Gaussian intrinsic lineshape with the linewidth shown alongside the curves. Right: composite spectra calculated assuming isolated and clustered Gd^{3+} ions, with the clustered fraction indicated in the figure. The intrinsic lineshape for the isolated ions is Gaussian, with the linewidth $\Delta_B = 5$, 10 and 15 mT for the (1), (2) and (3) curves, respectively. The clusters are described by a Gaussian lineshape with $g_{\text{eff}} = 2.25$ and $\Delta_B = 95$ mT.

in the environment of the Gd^{3+} sites and (iii) departure from a random spatial distribution of these sites in the glass network (clustering etc). Figure 5 (left) shows that the spectral transformations in the high-field range observed at higher gadolinium concentrations cannot be ascribed exclusively to dipole–dipole broadening; indeed, the spectra calculated under such an assumption have too intense low-field features. One can see from figure 4 that the relative intensity of the latter features is reduced at lower σ_0-values, i.e. for more ordered Gd^{3+} sites. However, in this case the high-field feature becomes very narrow and is located exactly at $g_{\text{eff}} = 2.00$, whereas in the experimental EPR spectra of the Gd3 and Gd4 glasses, the corresponding feature is very broad and manifestly shifted to lower magnetic fields.

Finally, a good fit to the whole EPR spectra of these glasses could be obtained only by superposing a (broadened) signal due to isolated Gd^{3+} ions and a broad resonance with $g_{\text{eff}} \approx 2.25$, see figure 5 (right). The latter signal can be ascribed to clusters of Gd^{3+} ions, linked with each other by exchange interaction through the oxygen bridges. This finding is consistent with the Weiss constant values found for the Gd3 and Gd4 glasses as well as with the increase of high-temperature Gd^{3+} effective magnetic moments. With the increased relative number of clustered gadolinium ions in the Gd3 and, even more, in the Gd4 glass, the effect of the CF on the average magnetic parameters is expected to weaken. Indeed, the resonance of clustered Gd^{3+} ions occurs much closer to the free-electron value for the effective g-factor than for the isolated gadolinium ions that prevail at lower doping levels.

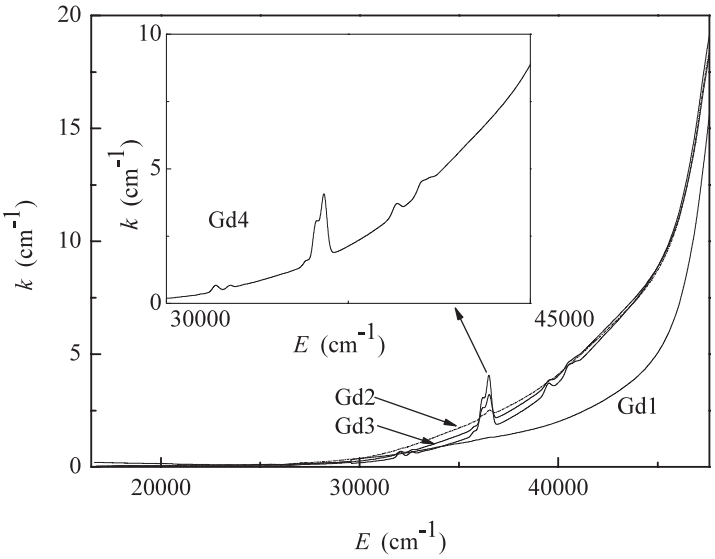

Figure 6. Absorption spectra for Gd1–Gd4 glasses at room temperature. The inset shows the region of the f–f transitions for Gd4 glass.

3.3. Optical spectroscopy

The optical absorption spectra shown in figure 6 are markedly different for the Gd1 sample and for all other samples. In the first case, the absorption is due to the basic glass components and La; the gadolinium contribution to the absorption is negligible because of its low content. In the second case, the change in shape of the absorption spectra and their shift to lower photon energies can be ascribed to the presence of Gd^{3+} ions. The first strong f–d transition inside the Gd3 ion occurs at about 75×10^3 cm^{-1} [20], i.e. deeply inside the fundamental absorption band. Therefore, non-monotonic dependence of the strong absorption band edge position on the gadolinium concentration suggests that the extra absorption is due not only to a charge transfer between gadolinium and oxygen but also to a charge transfer between Gd^{3+} ions or between Gd^{3+} and La^{3+} ions, similar to what has been assumed for glasses activated by Pr^{3+} [21]. This assumption is consistent with the above conclusion about the formation of rare-earth clusters.

A part of the absorption spectrum in the region of some f–f transitions is shown in the inset to figure 6. Three groups of lines corresponding to the multiplet-to-multiplet transition manifolds $^8S_{7/2} \rightarrow {}^6P_J$, $^8S_{7/2} \rightarrow {}^6I_J$ and $^8S_{7/2} \rightarrow {}^6D_J$ are distinguished on the background of the fundamental absorption band edge. The strongest one (corresponding to the transitions $^8S_{7/2} \rightarrow {}^6I_J$) is observed for the samples Gd2–Gd4 in the vicinity of the photon energy 36×10^3 cm^{-1}. Three components are resolved in this region, similar to Gd^{3+} spectra in borate [22] and alkali zinc boro-sulphate [23] glasses (see table 1), while in glasses and compounds based on fluorine or chlorine, four lines are usually resolved (see for instance [24–28]). In order to obtain the concentration dependence of the spectral position and the oscillator strength of these components, the contribution of the strong absorption (well described by the Urbach rule) was subtracted from the total absorption. The remaining absorption has been decomposed into three Gaussian curves, on the grounds of the observable features. The Gaussian function is the most appropriate one for a description of the non-homogeneously broadened absorption lines [29] in the glasses. Such decomposition (see the example in

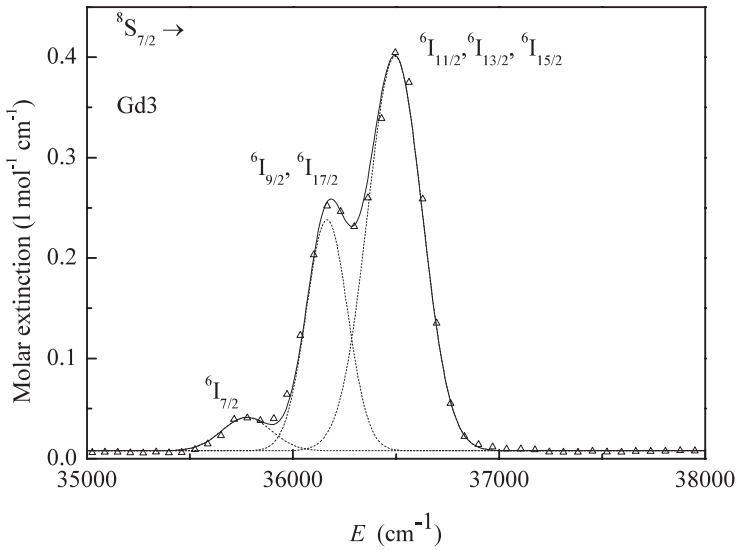

Figure 7. Decomposition of the $^8S_{7/2} \rightarrow {}^6I_J$ absorption band into three lines in agreement with the observed spectral features for the Gd3 sample at 300 K. The triangles are experimental points and the solid line is the sum of the three components shown by the dashed curves.

Table 1. Energies and oscillator strengths of f–f bands in Gd2–Gd4 glasses.

Transition	Energy (cm^{-1})		Oscillator strength		
$^8S_{7/2} \rightarrow$	Gd2	Gd3, Gd4	Gd2	Gd3	Gd4
$\rightarrow {}^6I_{7/2}$	35 715	35 775	4.26×10^{-8}	4.32×10^{-8}	4.26×10^{-8}
$\rightarrow {}^6I_{9/2}, {}^6I_{17/2}$	36 160	36 165	2.71×10^{-7}	2.49×10^{-7}	2.46×10^{-7}
$\rightarrow {}^6I_{11/2}, {}^6I_{15/2}, {}^6I_{13/2}$	36 495	36 495	5.23×10^{-7}	5.63×10^{-7}	5.61×10^{-7}

figure 7 for Gd3) adequately fits the experimental spectra for all three Gd2–Gd4 glasses. The oscillator strengths were calculated using the relationship [30]

$$f = 4.318 \times 10^{-9} \int \varepsilon(k)\,\mathrm{d}k = 4.318 \times 10^{-9} I \tag{2}$$

where $\varepsilon(k)$ is the decimal molar extinction coefficient for the wavenumber k (cm^{-1}) and I is the line intensity.

The component energies and oscillator strengths given in table 1 are for the Gd2–Gd4 glasses. In contrast to the strong absorption band edge, only small changes in the f–f band characteristics are observed between Gd2 and Gd3 or Gd4 glasses. For the two latter samples these characteristics practically coincide, while the strong absorption band tail (in the region (30–45) $\times 10^3$ cm^{-1} in figure 6) is very different. The main difference between Gd2 and Gd3 (Gd4) is a shift towards higher energies of the transition between levels with the *same* J-value, $^8S_{7/2} \rightarrow {}^6I_{7/2}$. This difference, though minor, is beyond the errors of the measurements and the spectral decomposition, so it is indicative of certain changes in the Gd^{3+} environment arising with the increase of the Gd_2O_3 content. Since an electron energy level is determined by the CF strength, and, as a rule, it is higher for lower CF, one can suppose CF in Gd3 and Gd4 to be weaker than in Gd2. The CF strength reduction can be due to the La substitution for Gd as mentioned above in relation to the change of effective magnetic moment. In principle, the

intensity changes of the f–f bands can be ascribed to the Gd clustering because these transitions are spin forbidden. But the exchange interaction is too low in the present case; besides, the character of changes in the f–f bands differs from that for the strong absorption.

4. Conclusion

In gadolinium-containing oxide glasses, the Gd^{3+} ions occupy well-defined sites. A computer-assisted EPR study has shown that, in comparison with other gadolinium-containing glasses, in the glasses $x Gd_2O_3$–$(51.35 - x)La_2O_3$–$17.4Al_2O_3$–$12.4B_2O_3$–$18.85(SiO_2 + GeO_2)$, the local environment of the Gd^{3+} ions is less ordered. The onset of clustering occurs for x-values about 5 mass% Gd_2O_3, as evidenced by both magnetization and EPR measurements.

Several peculiarities are revealed in the magnetic and optical properties of these glasses:

(1) positive Weiss constants for samples with relatively high Gd_2O_3 concentrations,
(2) deviation from monotonic magnetization field dependence for the sample with the maximum Gd concentration (10 mass% of Gd_2O_3),
(3) lower relative intensity of the $g_{\text{eff}} = 2.0$ EPR spectral component in comparison with other gadolinium-containing glasses, and
(4) changes in the strong absorption band edge and in certain f–f band positions and intensities with Gd content.

These peculiarities testify to changes of the Gd^{3+} environment in the glass network as a function of gadolinium concentration and to the occurrence of Gd clusters with an increase in doping level.

References

[1] Chepeleva I V and Lazukin V N 1976 *Dokl. Akad. Nauk SSSR* **226** 311
[2] Brodbeck C M and Iton L E 1985 *J. Chem. Phys.* **83** 4285
[3] Čugunov L, Mednis A and Kliava J 1991 *J. Phys.: Condens. Matter* **3** 8017
[4] Ardelean I, Burzo E, Mîţulescu-Ungar D and Simon S 1992 *J. Non-Cryst. Solids* **146** 256
[5] Culea E and Milea I 1995 *J. Non-Cryst. Solids* **189** 246
[6] Culea E, Pop A and Cosma I 1996 *J. Magn. Magn. Mater.* **157/158** 163
[7] Legein C, Buzaré J Y, Silly G and Jacoboni C 1996 *J. Phys.: Condens. Matter* **8** 4339
[8] Ristoiu T, Culea E and Bratu I 1999 *Mater. Lett.* **41** 135
[9] Azzoni C B, Martino D, Paleari A, Speghini A and Bettinelli M 1999 *J. Mater. Sci.* **34** 3931
[10] Simon S, Ardelean I, Filip S, Bratu I and Cosma I 2000 *Solid State Commun.* **116** 83
[11] Smirnov A I and Sen S 2001 *J. Chem. Phys.* **115** 650
[12] Griscom D L 1980 *J. Non-Cryst. Solids* **40** 211
[13] Malakhovskii A V, Edelman I S, Radzyner Y, Yeshurun Y, Potseluyko A M, Zarubina T V, Zamkov A V and Zaitzev A I 2003 *J. Magn. Magn. Mater.* **263** 161
[14] Moon R M and Koehler W C 1975 *Phys. Rev.* B **11** 1609
[15] Ohtani T, Chevalier B, Lejay P, Vlasse M and Hagenmuller P 1983 *J. Appl. Phys.* **54** 5928
[16] Shannon R D 1976 *Acta Crystallogr.* A **32** 751
[17] Kliava J and Berger R 2003 *Recent Research Developments in Non-Crystalline Solids* vol 2 (Kerala: Transworld Research Network) at press
[18] Zheng W-C 2001 *Physica* B **304** 137
[19] James F 1990 *Comput. Phys. Commun.* **60** 329
[20] Borrelli H F 1964 *J. Chem. Phys.* **41** 3289
[21] Zabluda V, Pozeluyko A, Edelman I, Malakhovskii A, Zarubina T, Petrovskii G and Ivanov M 1998 *J. Magn. Magn. Mater.* **185** 207
[22] Verwey J W M, Imbusch G F and Blasse G 1989 *J. Phys. Chem. Solids* **50** 813
[23] Sreedhar B, Lakshmana Rao J, Narendra G L and Lakshman S V J 1992 *J. Phys. Chem. Solids* **59** 67
[24] Gilfanov F Z, Drabkina Zh S, Stolov A L and Livanova D D 1966 *Opt. Spectrosk.* **20** 282

[25] Caspers H H, Miller S A, Rast H E and Fry J L 1969 *Phys. Rev.* **180** 329
[26] Carnall W T, Fields P R and Sarup R 1971 *J. Chem. Phys.* **54** 1476
[27] Stephens E M, Metcalf D H, Berry M T and Richardson F S 1991 *Phys. Rev.* B **44** 9895
[28] Binnemans K, Gorller-Walrand C and Adam J L 1997 *Chem. Phys. Lett.* **280** 333
[29] Stoneham A M 1969 *Rev. Mod. Phys.* **41** 82
[30] Carnall W T, Fields P R and Rajnak K 1968 *J. Chem. Phys.* **49** 4412